Supporting Information

Manganese oxide as a water-oxidizing catalyst: From bulk to Ångström-scale

Mohammad Mahdi Najafpour,[a,b]* Mohsen Abbasi Isaloo,[a] Mahnaz Abasi[a] and Małgorzata Hołyńska[c]

[a]*Department of Chemistry, Institute for Advanced Studies in Basic Sciences (IASBS), Zanjan, 45137-66731, Iran.*
[b] *Center of Climate Change and Global Warming, Institute for Advanced Studies in Basic Sciences (IASBS), Zanjan, 45137-66731, Iran.*
[c]*Fachbereich Chemie and Wissenschaftliches Zentrum für Materialwissenschaften (WZMW), Philipps-Universität Marburg, Hans-Meerwein-Straße, D-35032 Marburg, Germany.*
**Corresponding Author:*
Phone: (+98) 241 415 3201. E-mail: mmnajafpour@iasbs.ac.ir

Table of Contents

Title	*Page*
The $CaMn_4O_5$ cluster and the surrounding amino acids	***4***
Set-up for electrochemical water oxidation	**5**
TEM Images	**6-9**
BET diagrams	**10-17**
X-ray diffraction analysis – Complex 1	**18-28**
Proposed mechanisms for the self-healing	**29**
References	**30**

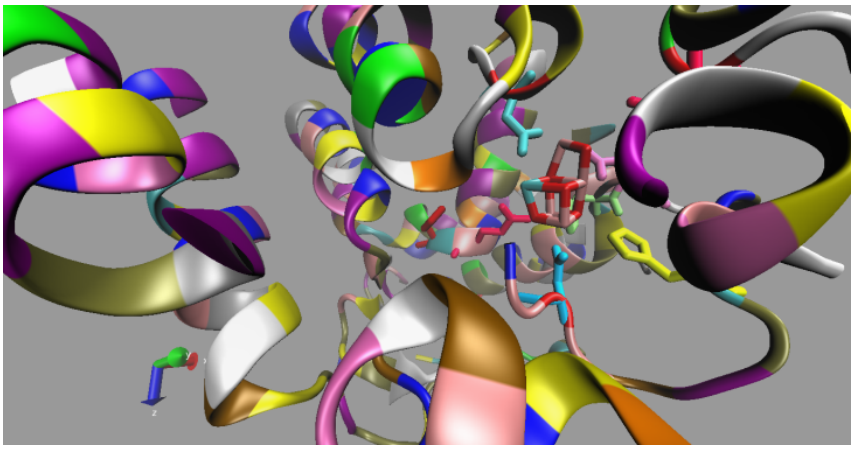

a

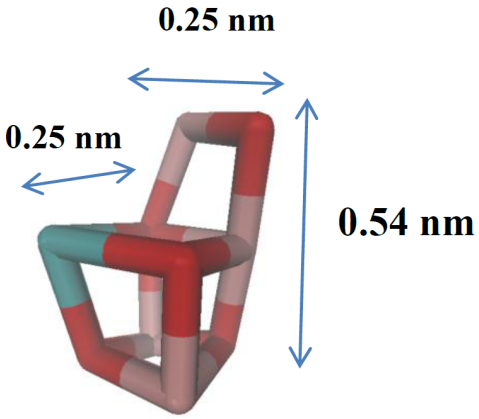

b

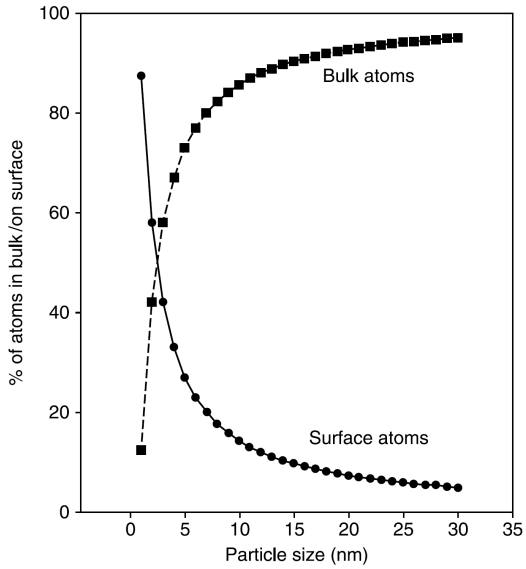

c

Fig. S1 The $CaMn_4O_5$ cluster and the surrounding amino acids in PSII (a). The $CaMn_4O_5$ cluster in PSII that has dimensions of about ~ 0.5 × 0.25 × 0.25 nm^3 (oxygen: red; Mn: pink and calcium: grey) (b). These images were made with VMD software and are owned by the Theoretical and Computational Biophysics Group, NIH Resource for Macromolecular Modeling and Bioinformatics, at the Beckman Institute, University of Illinois at Urbana-Champaign. The original data are taken from from the ref. S1 (PDB: 3ARC). Calculated surface to bulk atomic ratio (c). Image c reprinted with permission from ref. S2 Copyright (1996) by American Chemical Society.

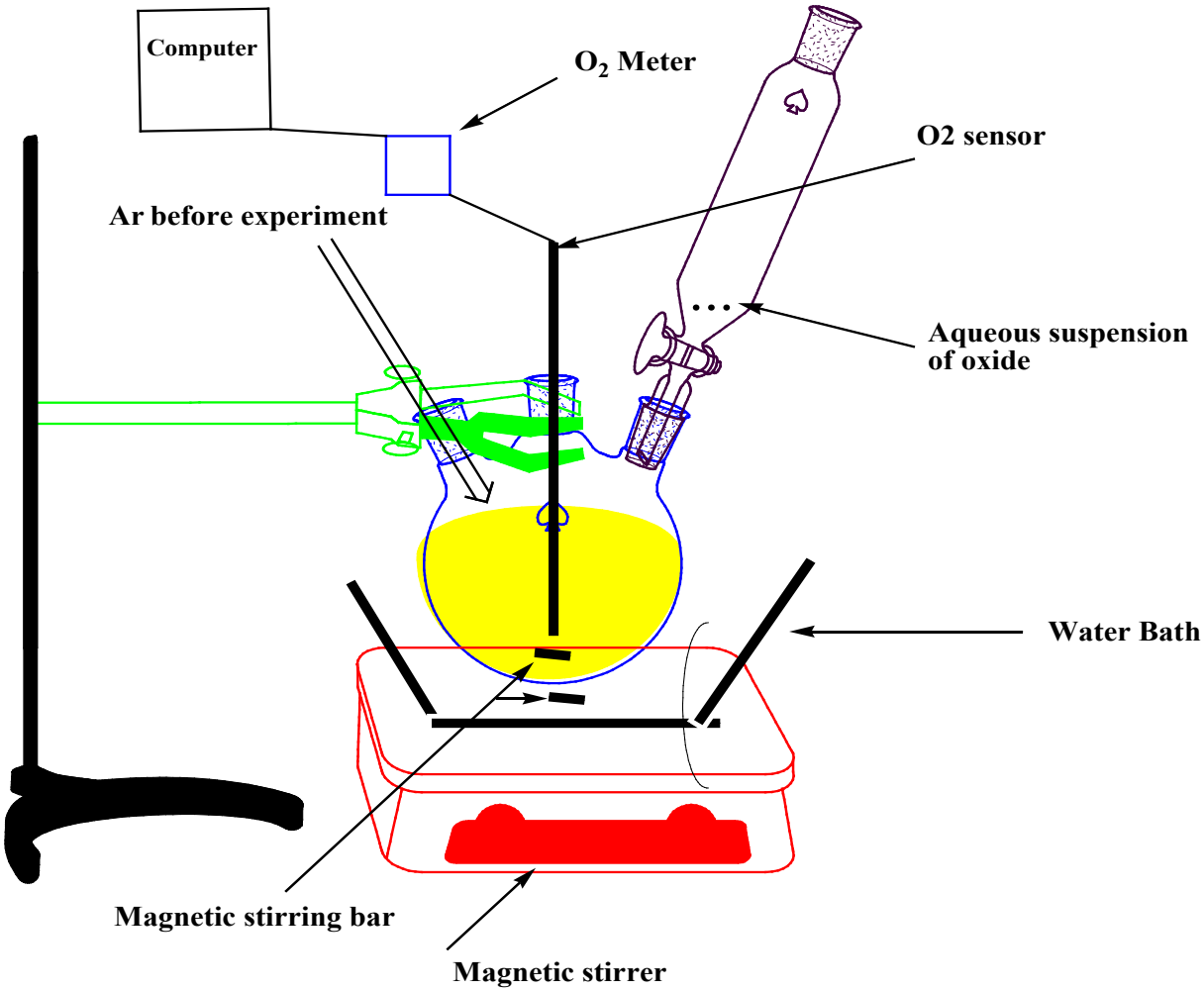

Fig. S2 The reactor set-up for oxygen evolution experiment from aqueous solution in the presence of Ce(IV) and catalysts.

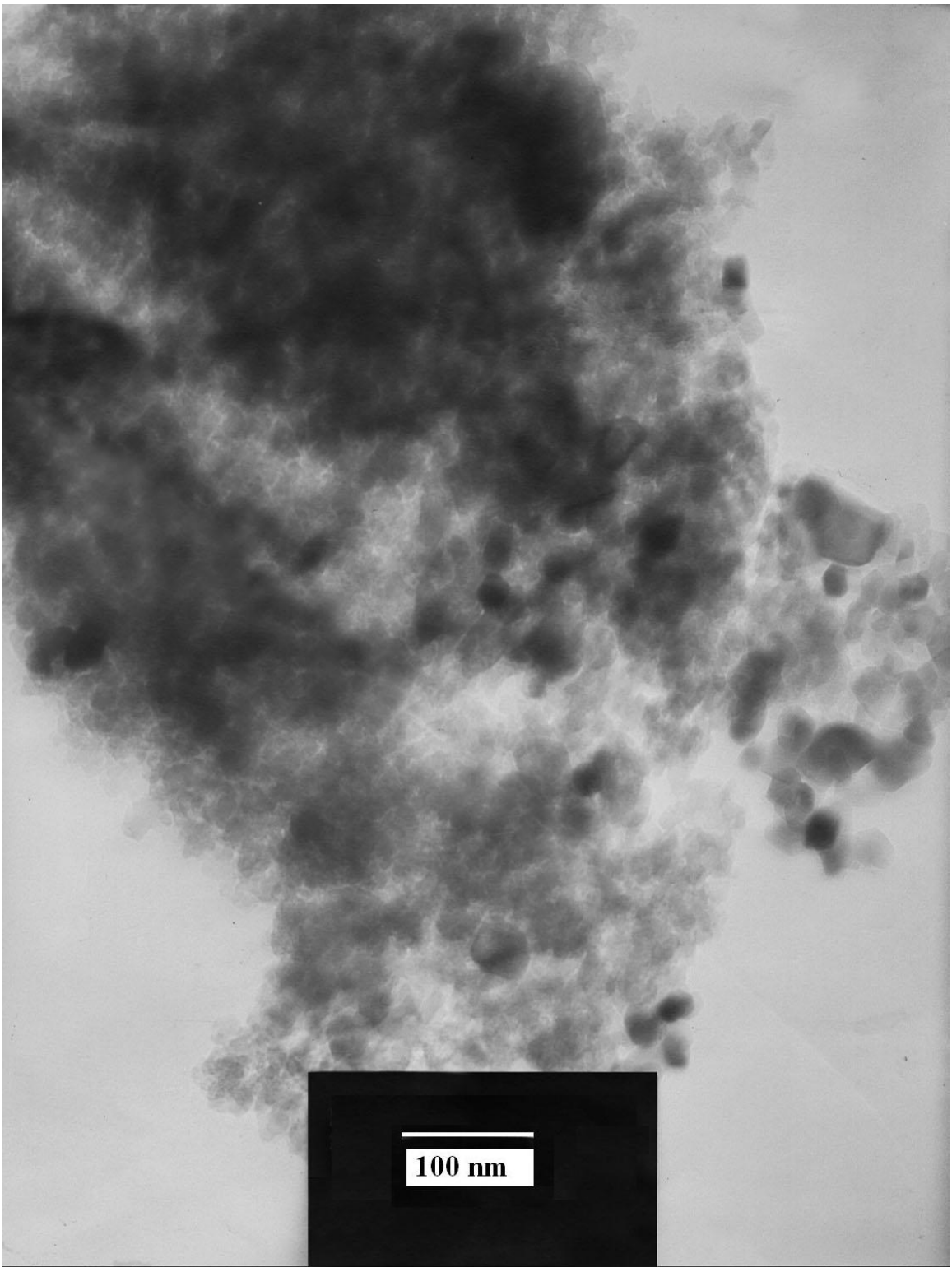

a

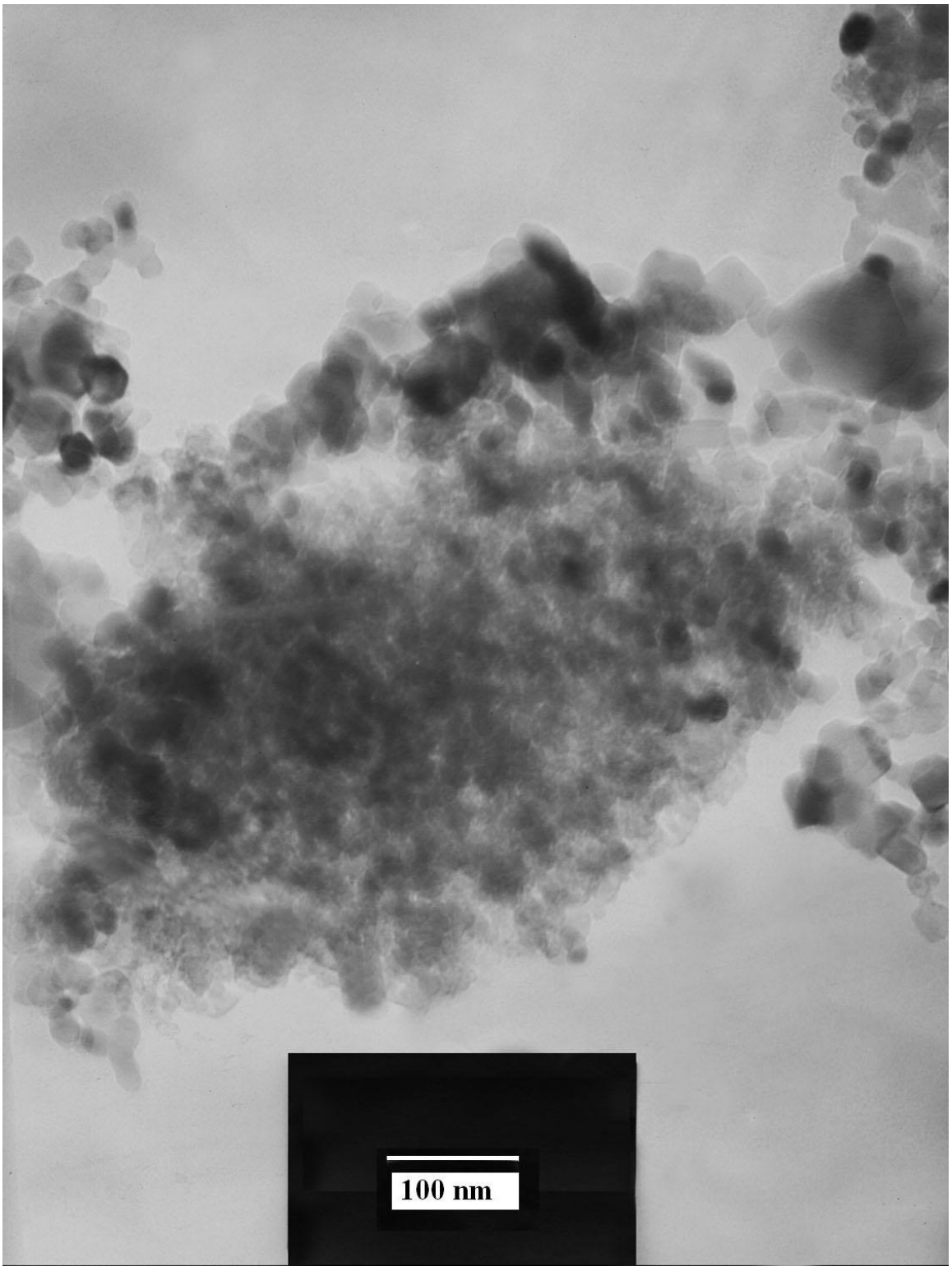

b

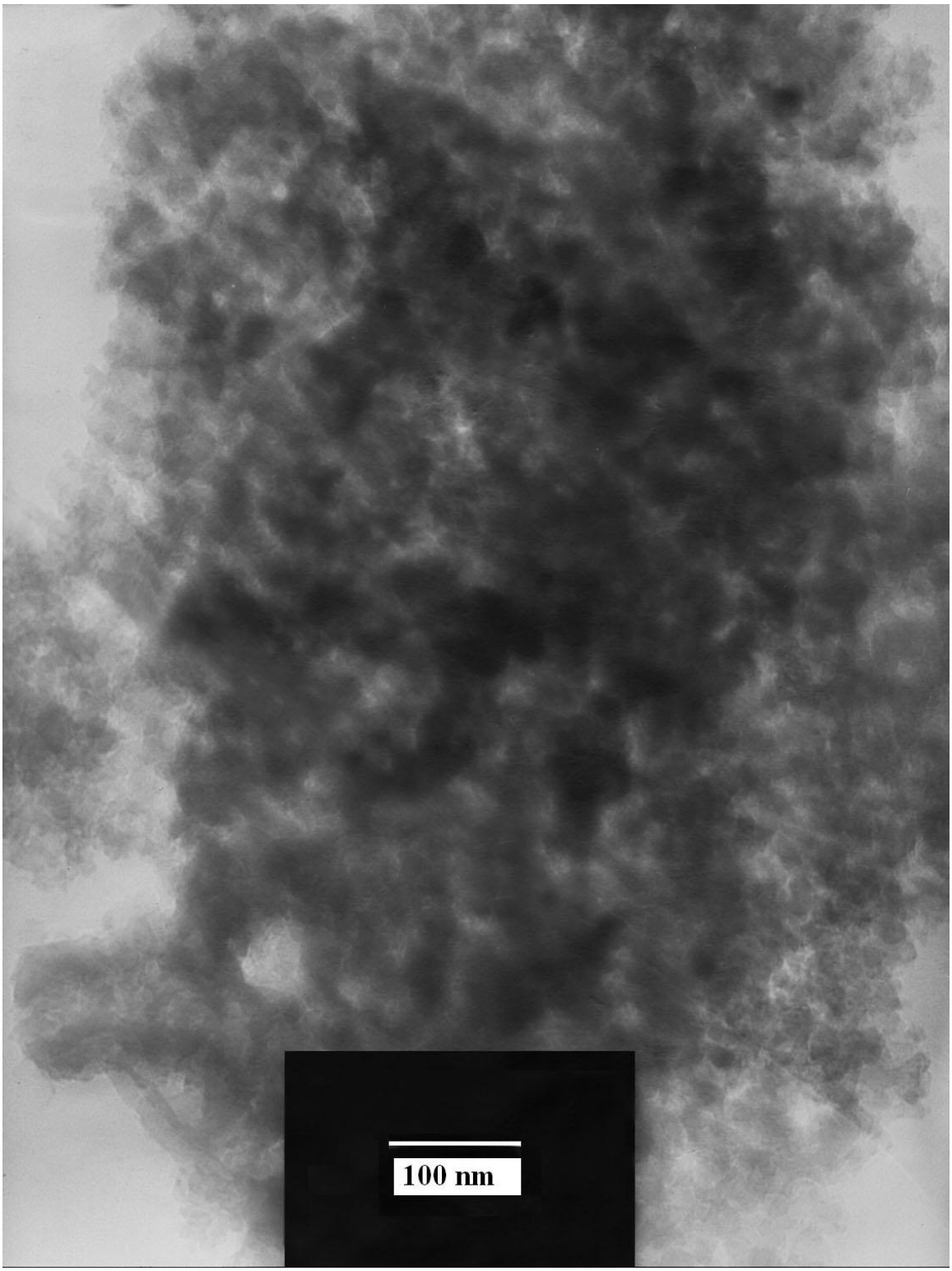

c

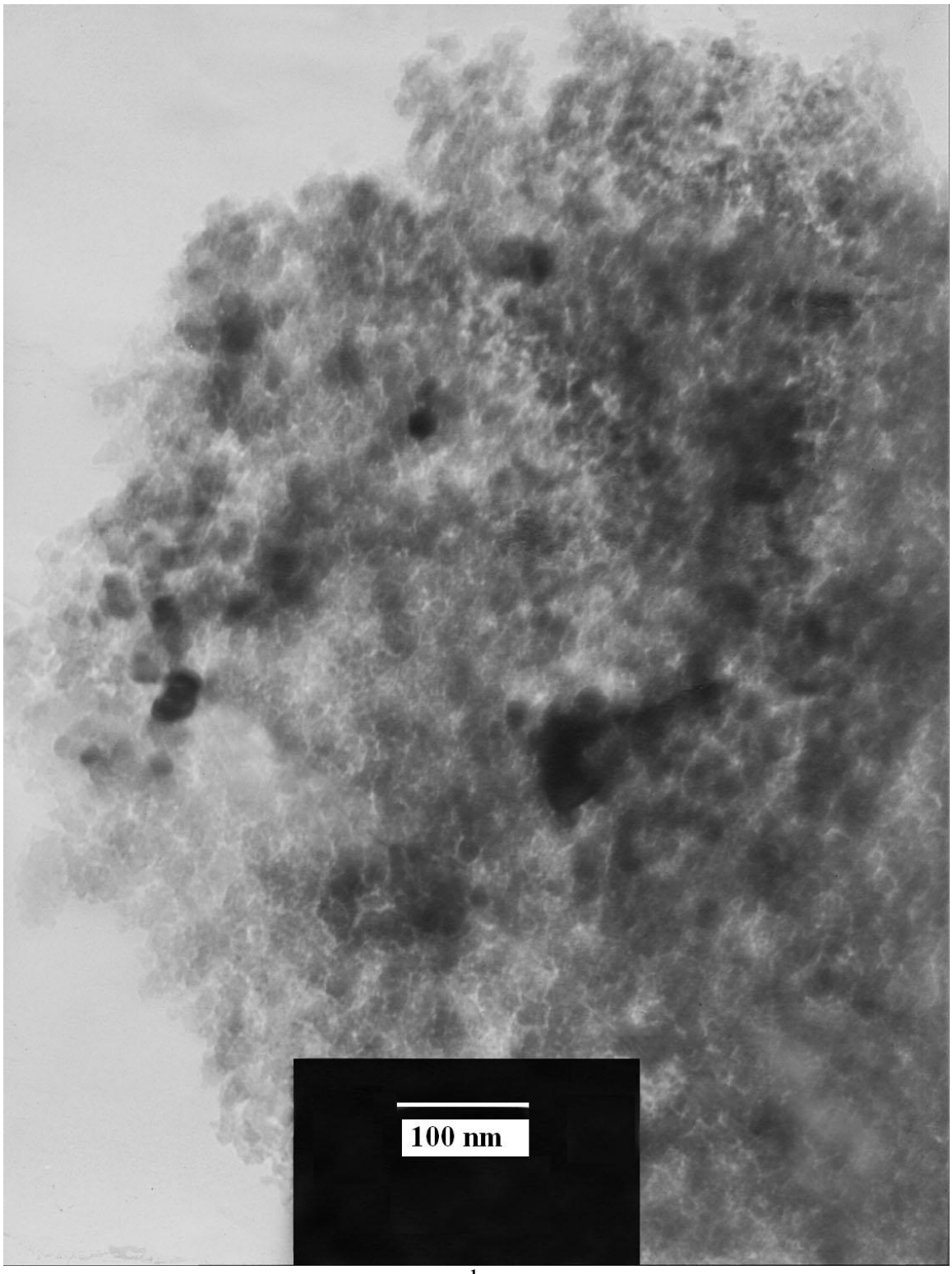

d

Fig. S3 TEM images of manganese oxides within Faujasite zeolite (manganese: 0.15 %) (a-d).

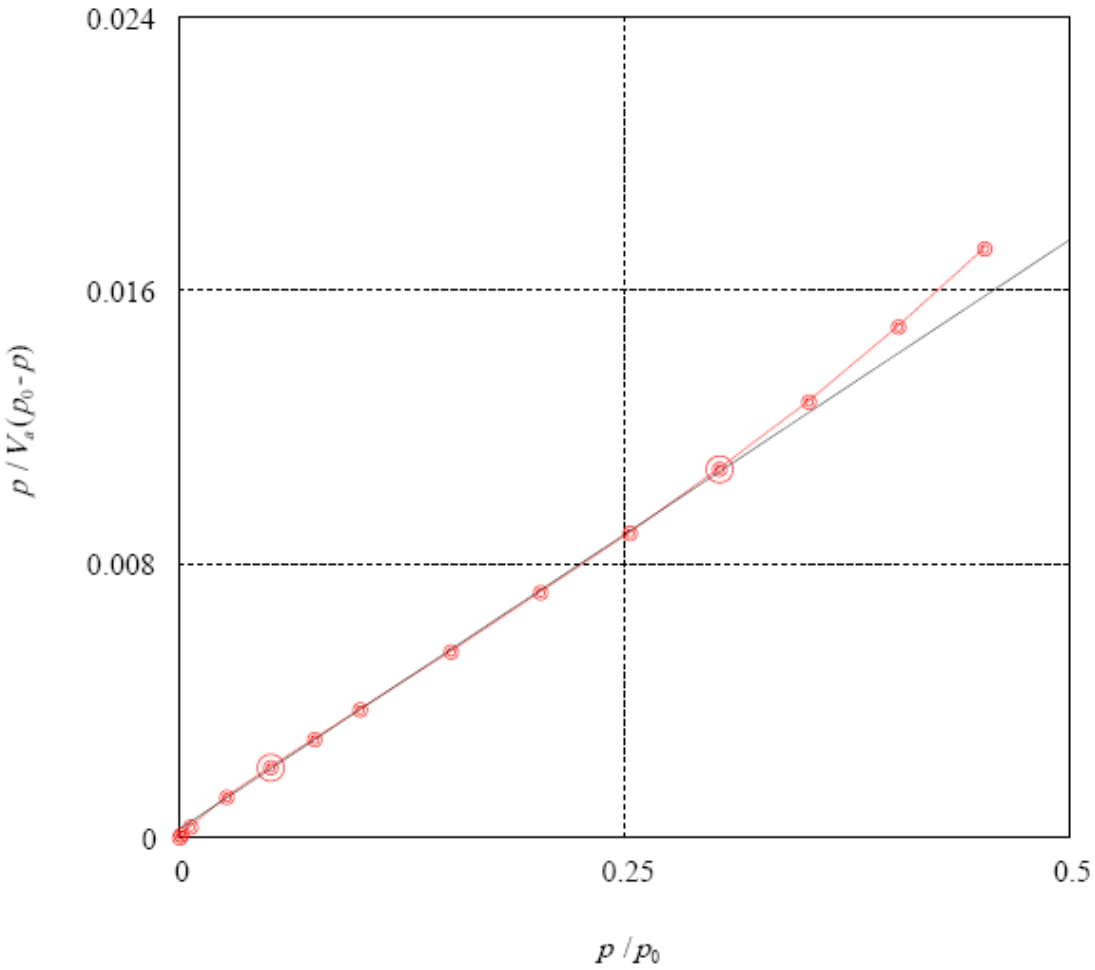

BET-Plot

Adsorptive N2

Adsorption temperature 77 [K]

P1-Zeolite HY.DAT

P1-Zeolite HY
Mirzaie
pretreatment-4h-100 degree

Sample weight	7.8600E-02	[g]	Date of measurement	13/07/10	
Saturated vapor pressure	106.94	[kPa]	Time of measurement	13:42:28	

V_m	28.850	[cm^3(STP) g^{-1}]	$a_{s,BET}$	1.2557E+02	[m^2 g^{-1}]
C	138.11		Total pore volume(p/p_0=0.990)	0.5144	[cm^3 g^{-1}]
Mean pore diameter	16.386	[nm]			

Fig. S4 BET diagram for the HY zeolite.

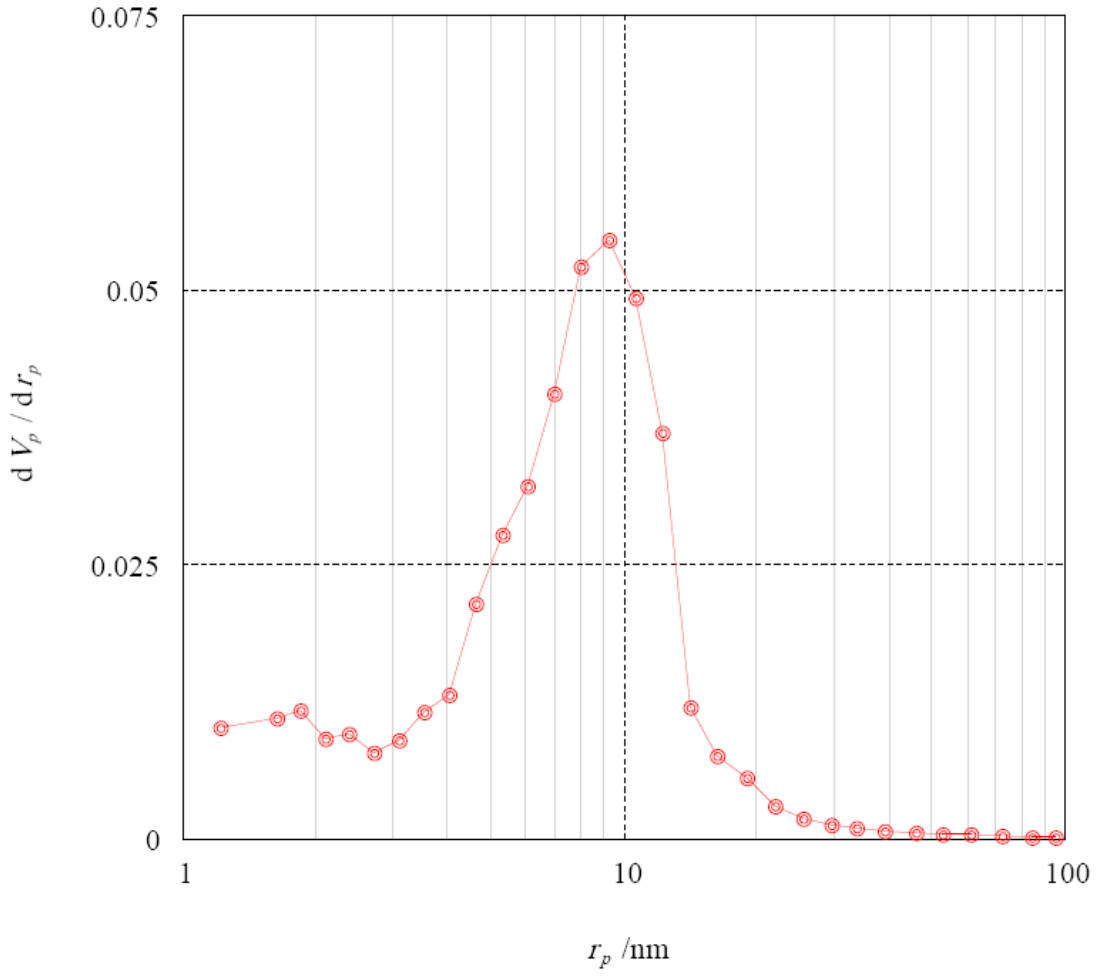

BJH-Plot

Adsorption branch

Adsorptive N2

Adsorption temperature 77 [K]

◎ P1-Zeolite HY.DAT

P1-Zeolite HY
Mirzaie
pretreatment-4h-100 degree

Sample weight	7.8600E-02	[g]		Date of measurement	13/07/10
Saturated vapor pressure	106.94	[kPa]		Time of measurement	13:42:28

V_p	0.5104	[$cm^3\ g^{-1}$]	$r_{p,peak}(Area)$	9.23	[nm]
a_p	130.56	[$m^2\ g^{-1}$]			

Fig. S5 BJH diagram for the HY zeolite.

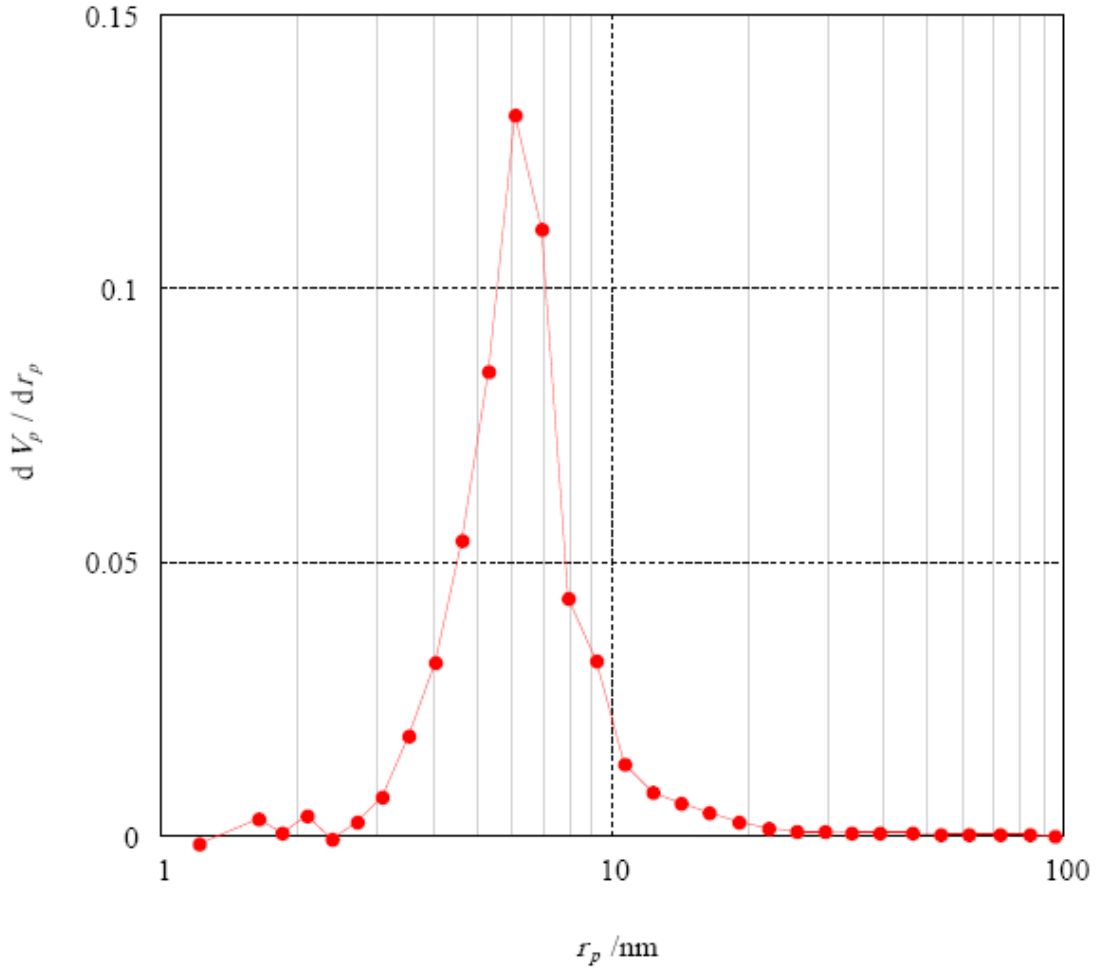

DH-Plot

Desorption branch

Adsorptive N2

Adsorption temperature 77 [K]

● P1-Zeolite HY.DAT

P1-Zeolite HY
Mirzaie
pretreatment-4h-100 degree

Sample weight	7.8600E-02	[g]	Date of measurement	13/07/10
Saturated vapor pressure	106.94	[kPa]	Time of measurement	13:42:28

V_p	0.5252	[$cm^3\ g^{-1}$]	$r_{p,peak}$ (*Area*)	6.06	[nm]
a_p	153.11	[$m^2\ g^{-1}$]			

Fig. S6 DH diagram for the HY zeolite.

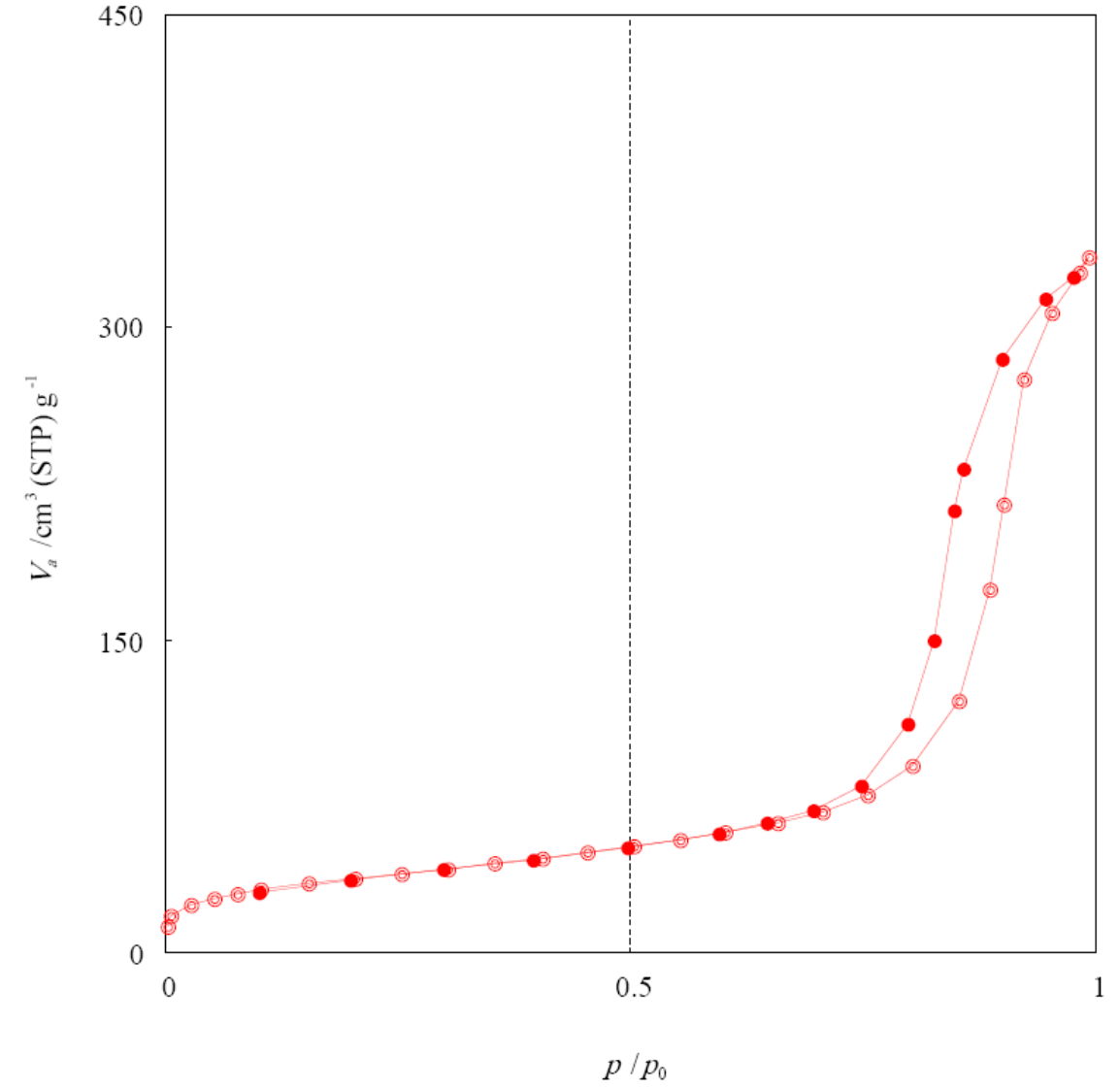

Adsorption / desorption isotherm

Adsorptive N2

Adsorption temperature 77 [K]

P1-Zeolite HY.DAT

P1-Zeolite HY
Mirzaie
pretreatment-4h-100 degree

Sample weight	7.8600E-02	[g]	Date of measurement	13/07/10
Saturated vapor pressure	106.94	[kPa]	Time of measurement	13:42:28

Fig. S7 Adsorption / Desorption Isotherm diagram for the HY Zeolite.

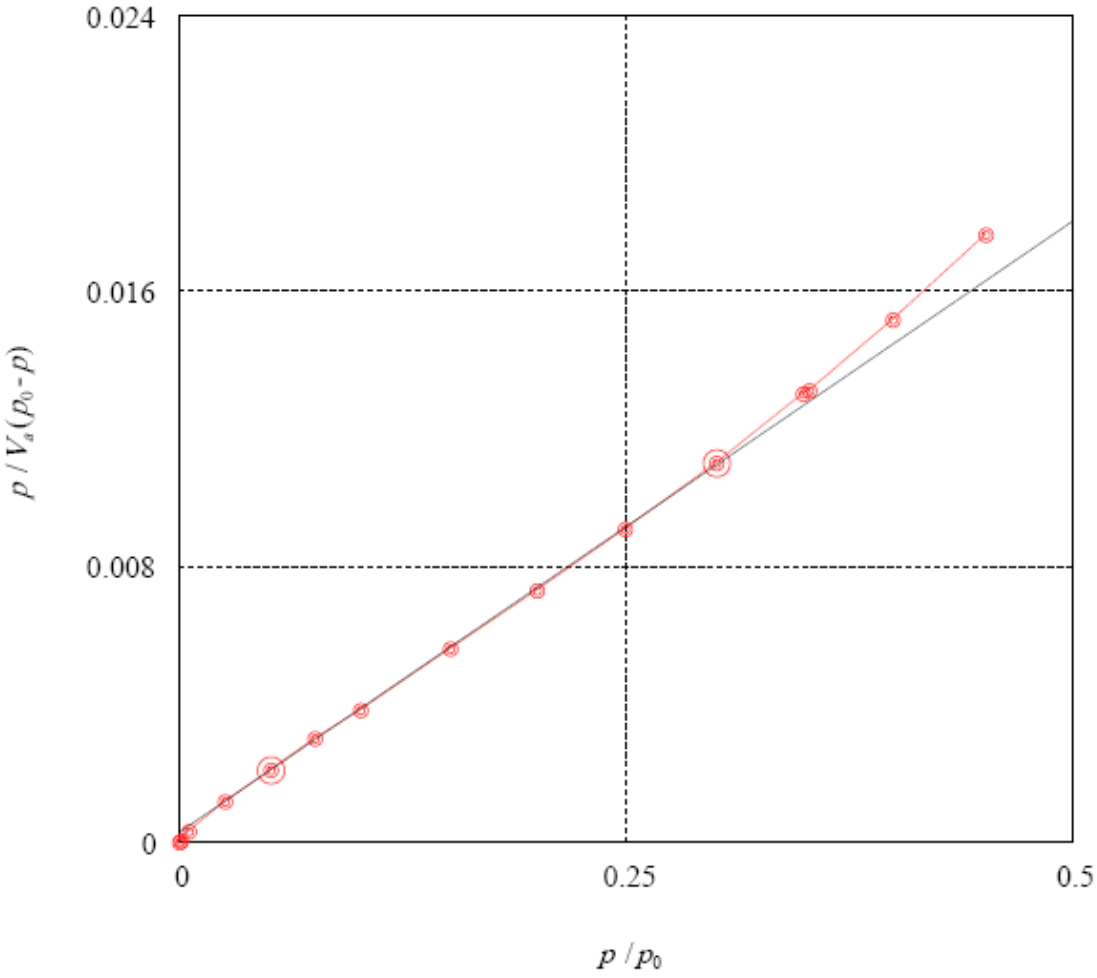

BET-Plot

Adsorptive N2

Adsorption temperature 77 [K]

P1-4-30.DAT

P1-4-30
Mirzaie
pretreatment-4h-100degree

Sample weight	3.2100E-02	[g]	Date of measurement	13/07/10	
Saturated vapor pressure	106.72	[kPa]	Time of measurement	11:42:15	

V_m	27.949	[cm^3(STP) g^{-1}]	$a_{s,BET}$	1.2165E+02	[m^2 g^{-1}]
C	134.27		Total pore volume(p/p_0=0.990)	0.5085	[cm^3 g^{-1}]
Mean pore diameter	16.721	[nm]			

Fig. S8 BET diagram for manganese oxide within the HY zeolite with Mn content of 0.4 wt %.

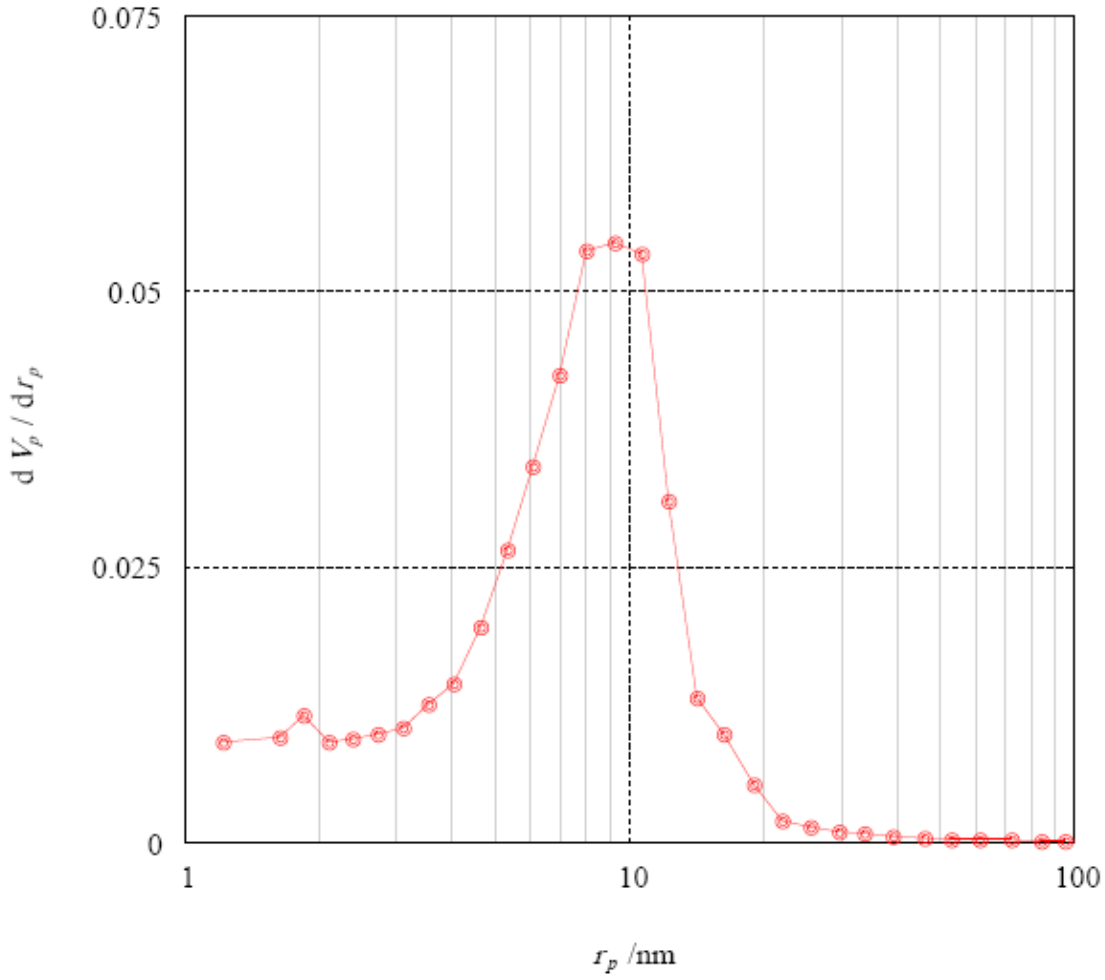

BJH-Plot

Adsorption branch

Adsorptive N2

Adsorption temperature 77 [K]

P1-4-30.DAT

P1-4-30
Mirzaie
pretreatment-4h-100degree

Sample weight	3.2100E-02	[g]	Date of measurement	13/07/10
Saturated vapor pressure	106.72	[kPa]	Time of measurement	11:42:15

V_p	0.5064	[cm^3 g^{-1}]	$r_{p,peak}$ (*Area*)	9.23	[nm]
a_p	130.81	[m^2 g^{-1}]			

Fig. S9 BJH diagram for manganese oxide within the HY zeolite with Mn content of 0.4 wt %.

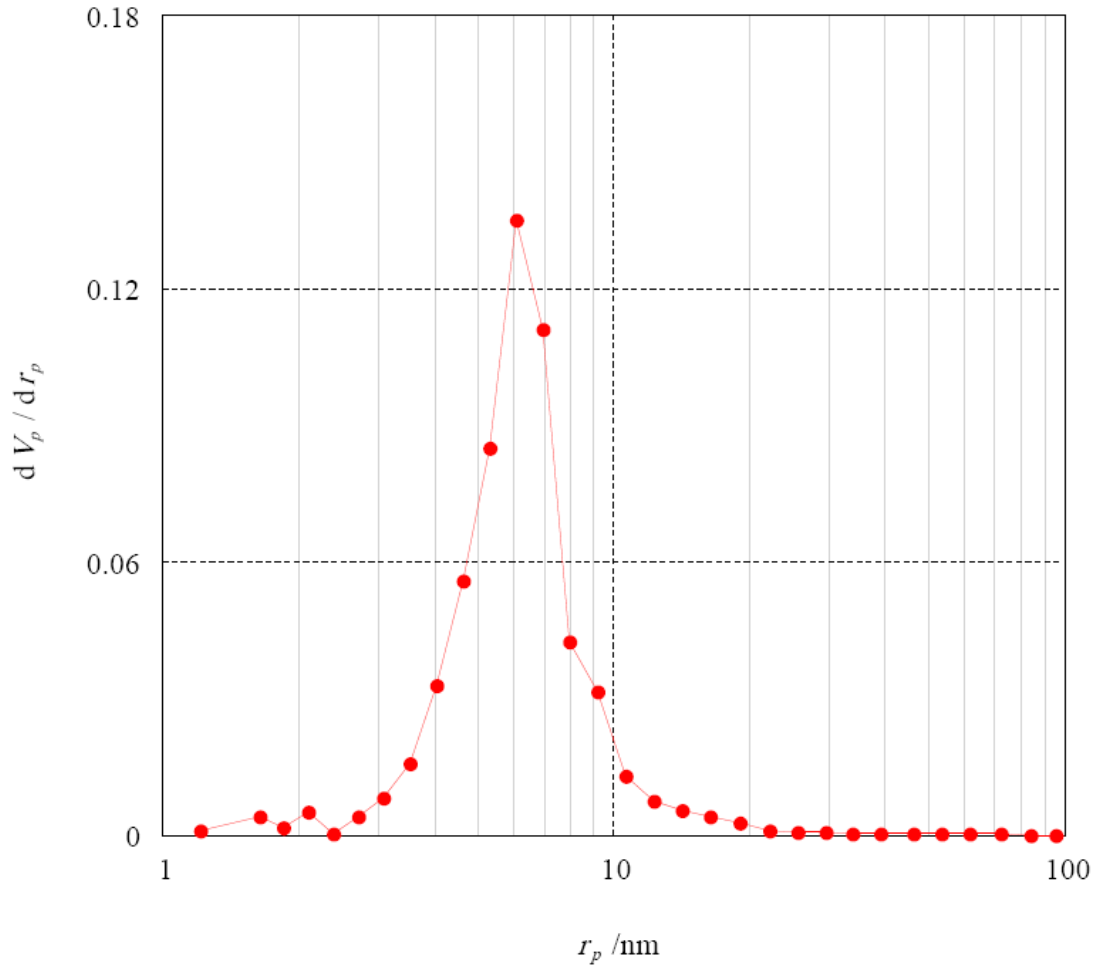

DH-Plot

Desorption branch

Adsorptive N2

Adsorption temperature 77 [K]

P1-4-30.DAT

P1-4-30
Mirzaie
pretreatment-4h-100degree

Sample weight	3.2100E-02	[g]		Date of measurement	13/07/10
Saturated vapor pressure	106.72	[kPa]		Time of measurement	11:42:15

V_p	0.5206	[$cm^3\ g^{-1}$]	$r_{p,peak}$(*Area*)	6.06	[nm]
a_p	157.25	[$m^2\ g^{-1}$]			

Fig. S10 DH diagram for manganese oxide within the HY zeolite with Mn content of 0.4 wt %.

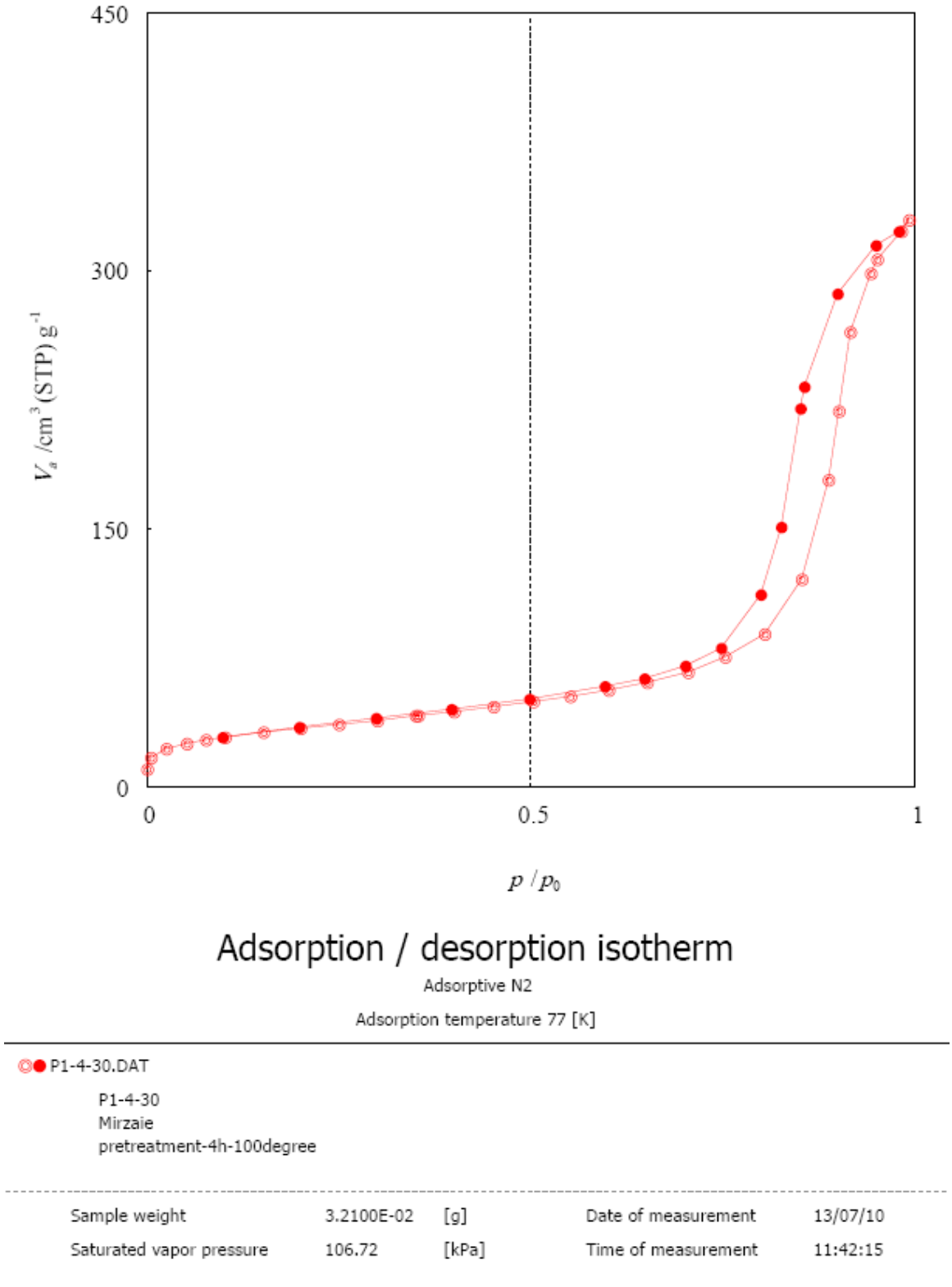

Fig. S11 Adsorption / Desorption Isotherm diagram for manganese oxide within the HY zeolite with Mn content of 0.4 wt %.

3. X-ray diffraction analysis – Complex 1

A monocrystal of complex **1** (see Article) suitable for X-ray diffraction analysis was chosen from a sample displaying twinning problems. Data collection was carried out on a Bruker Quest D8 device with microfocus MoK_{α} radiation and Photon 100 CMOS detector. Main crystallographic data are collected in Table S1.

The structure **1** was solved by direct methods in SHELXS97 and refined by full-matrix method in SHELXL97 [S3]. Three full-occupancy water molecules of solvation were located. For other six water molecules (O4W-O6W, O8W-O10W) the occupancies were refined and subsequently fixed at half-values. O7W-molecule was modeled as disordered in two positions (O7W/O77W components) with occupancies refined to 0.60(3)/0.40(3), respectively. Water ligands bonded to Mn3 were found to be disordered in two positions related by a rotation with respect to an O-Mn-O axis, with occupancies refined to 0.74(2)/0.26(2), respectively. Both H atoms from O1W/O2W and one H atom from O3W water molecule were found on difference Fourier maps, refined with DFIX restraints setting O-H bond lengths at 0.820(2) and H…H distances at 1.50(1) Å, respectively, setting U_{eq} = 1.5U_{eq}(parent atom). Subsequently their coordinates were fixed. Positions of the two H atoms from the complex anion were calculated in the expected positions and a riding model was used with U_{eq} = 1.2U_{eq}(parent atom). ISOR restraints were used for all water O atoms and for the anion O8, O20 and O29 atoms.

On the final difference Fourier map the highest maximum of 2.67 e/Å^3 is situated at 2.80 Å from W1, 1.32 Å from O9W, 2.44 Å from O6W and 1.70 Å from O4. The maximum could be interpreted as sign of more complicated disorder of the solvent part. However, the distance to the anion terminal O4 atom is too close. O4 is not disordered, the W1-O4 bond length is in the

expected range, therefore the maximum cannot be assigned a plausible interpretation. Presence of such maxima might be connected with drawbacks of the absorption correction.

Table S1. Selected X-ray data for **1**.

	1
Formula	$H_{36}Mn_5O_{58}W_{12}\cdot 18(H_2O)$
Formula weight	3769.48
Temperature [K]	100(2)
λ [Å]	0.71073
Crystal system	Triclinic
Space group	Pī
a [Å]	11.350 (3)
b [Å]	12.153 (3)
c [Å]	14.391 (4)
α [°]	65.37 (3)
β [°]	66.76 (3)
γ [°]	80.51 (3)
V [Å^3]	1658.0 (8)
Z, ρ_{calc} [g cm^{-3}]	1, 3.775
μ [mm^{-1}]	21.76
F(000)	1693
Crystal size [mm]	0.5 × 0.04 × 0.03
θ range[°]	2.69-25.00
rflns: total/unique	16997/ 5696
R(int)	0.046
Abs. corr.	numerical
Min., max. transmission factors	0.196, 0.753
Data/restraints/params	5696/84/462
GOF on F^2	1.02
R1 [$I > 2\sigma(I)$]	0.032
wR_2 (all data)	0.079
Max., min. $\Delta\rho_{elect}$ [e Å^{-3}]	2.67/-1.91

Table S2. Selected geometric parameters [Å, °] for **1**. Symmetry codes: (i) -*x*, -*y*+1, -*z*+1; (ii) -*x*, -*y*+2, -*z*+1; (iii) *x*, *y*+1, *z*; (iv) -*x*+1, -*y*+1, -*z*; (v) *x*, *y*-1, *z*.

W1—O5	1.753 (6)	W6—O17	1.740 (6)
W1—O4	1.768 (6)	W6—O18	1.781 (6)
W1—O2	1.874 (6)	W6—O3^{i}	1.881 (7)
W1—O3	1.979 (6)	W6—O16	1.916 (6)
W1—O14^{i}	2.136 (6)	W6—O13	2.194 (6)
W1—O1	2.181 (6)	W6—O1^{i}	2.349 (6)
W2—O9	1.747 (6)	Mn1—O22	2.155 (8)
W2—O19^{i}	1.795 (6)	Mn1—O5	2.162 (7)
W2—O1	1.885 (6)	Mn1—O26	2.162 (8)
W2—O8	1.945 (6)	Mn1—O23	2.180 (9)
W2—O6	2.223 (6)	Mn1—O25	2.203 (7)
W3—O12	1.725 (6)	Mn1—O24	2.224 (7)
W3—O10	1.884 (6)	Mn2—O9	2.142 (7)
W3—O7	1.893 (7)	Mn2—O4^{ii}	2.145 (7)
W3—O11	1.929 (6)	Mn2—O29	2.158 (7)
W3—O2	1.963 (6)	Mn2—O18^{iii}	2.176 (6)
W3—O6	2.259 (6)	Mn2—O28	2.189 (6)
W4—O15	1.732 (6)	Mn2—O27	2.199 (7)
W4—O14	1.814 (6)	Mn3—O20	2.151 (6)
W4—O13	1.919 (6)	Mn3—O20^{iv}	2.151 (6)
W4—O8	1.967 (6)	Mn3—O30^{iv}	2.164 (9)
W4—O10	2.068 (6)	Mn3—O30	2.164 (9)
W4—O6	2.241 (7)	Mn3—O31A^{iv}	2.184 (15)
W5—O21	1.732 (7)	Mn3—O31A	2.184 (15)
W5—O20	1.743 (6)	Mn3—O30A^{iv}	2.185 (16)
W5—O11	1.891 (6)	Mn3—O30A	2.185 (16)
W5—O16	1.949 (6)	Mn3—O31	2.199 (8)
W5—O19	2.203 (6)	Mn3—O31^{iv}	2.199 (8)
W5—O13	2.262 (6)		
O5—W1—O4	102.4 (3)	O16—W6—O1^{i}	84.4 (2)
O5—W1—O2	100.3 (3)	O13—W6—O1^{i}	77.4 (2)
O4—W1—O2	99.6 (3)	O22—Mn1—O5	96.9 (3)
O5—W1—O3	94.9 (3)	O22—Mn1—O26	91.9 (3)
O4—W1—O3	91.7 (3)	O5—Mn1—O26	89.4 (3)
O2—W1—O3	158.6 (3)	O22—Mn1—O23	88.3 (4)
O5—W1—O14^{i}	89.9 (3)	O5—Mn1—O23	174.0 (4)
O4—W1—O14^{i}	164.9 (3)	O26—Mn1—O23	93.4 (4)
O2—W1—O14^{i}	86.4 (2)	O22—Mn1—O25	92.0 (3)
O3—W1—O14^{i}	78.5 (2)	O5—Mn1—O25	86.3 (3)
O5—W1—O1	164.5 (2)	O26—Mn1—O25	174.5 (3)
O4—W1—O1	89.9 (3)	O23—Mn1—O25	90.6 (4)
O2—W1—O1	86.7 (3)	O22—Mn1—O24	169.0 (3)
O3—W1—O1	75.1 (2)	O5—Mn1—O24	93.9 (3)
O14^{i}—W1—O1	76.6 (2)	O26—Mn1—O24	90.5 (3)
O9—W2—O19^{i}	103.7 (3)	O23—Mn1—O24	80.9 (3)

O9—W2—O1	102.1 (3)	O25—Mn1—O24	86.4 (3)
O19^{i}—W2—O1	96.1 (3)	O9—Mn2—O4^{II}	172.3 (3)
O9—W2—O8	97.8 (3)	O9—Mn2—O29	91.8 (3)
O19^{i}—W2—O8	92.8 (3)	O4^{II}—Mn2—O29	92.0 (2)
O1—W2—O8	155.6 (3)	O9—Mn2—O18^{III}	85.9 (2)
O9—W2—O6	163.7 (3)	O4^{II}—Mn2—O18^{III}	91.3 (2)
O19^{i}—W2—O6	89.8 (3)	O29—Mn2—O18^{III}	171.7 (3)
O1—W2—O6	85.3 (3)	O9—Mn2—O28	88.5 (2)
O8—W2—O6	72.0 (2)	O4^{II}—Mn2—O28	84.9 (2)
O12—W3—O10	101.4 (3)	O29—Mn2—O28	86.8 (3)
O12—W3—O7	101.8 (3)	O18^{III}—Mn2—O28	101.1 (3)
O10—W3—O7	91.7 (3)	O9—Mn2—O27	93.9 (3)
O12—W3—O11	102.2 (3)	O4^{II}—Mn2—O27	93.1 (3)
O10—W3—O11	88.0 (3)	O29—Mn2—O27	86.1 (3)
O1—W2—O8	155.6 (3)	O9—Mn2—O18^{III}	85.9 (2)
O9—W2—O6	163.7 (3)	O4^{II}—Mn2—O18^{III}	91.3 (2)
O19^{i}—W2—O6	89.8 (3)	O29—Mn2—O18^{III}	171.7 (3)
O1—W2—O6	85.3 (3)	O9—Mn2—O28	88.5 (2)
O8—W2—O6	72.0 (2)	O4^{II}—Mn2—O28	84.9 (2)
O12—W3—O10	101.4 (3)	O29—Mn2—O28	86.8 (3)
O12—W3—O7	101.8 (3)	O18^{III}—Mn2—O28	101.1 (3)
O10—W3—O7	91.7 (3)	O9—Mn2—O27	93.9 (3)
O12—W3—O11	102.2 (3)	O4^{II}—Mn2—O27	93.1 (3)
O10—W3—O11	88.0 (3)	O29—Mn2—O27	86.1 (3)
O7—W3—O11	155.5 (3)	O18^{III}—Mn2—O27	86.1 (3)
O12—W3—O2	102.6 (3)	O28—Mn2—O27	172.6 (3)
O10—W3—O2	155.8 (3)	O20—Mn3—O20^{IV}	180.0
O7—W3—O2	86.7 (3)	O20—Mn3—O30^{IV}	93.1 (3)
O11—W3—O2	83.6 (3)	O20^{IV}—Mn3—O30^{IV}	86.9 (3)
O12—W3—O6	176.4 (3)	O20—Mn3—O30	86.9 (3)
O10—W3—O6	75.9 (2)	O20^{IV}—Mn3—O30	93.1 (3)
O7—W3—O6	76.0 (2)	O30^{IV}—Mn3—O30	179.999 (1)
O11—W3—O6	80.2 (2)	O20—Mn3—O31A^{IV}	86.8 (7)
O2—W3—O6	80.3 (3)	O20^{IV}—Mn3—O31A^{IV}	93.2 (7)
O15—W4—O14	103.4 (3)	O20—Mn3—O31A	93.2 (7)
O15—W4—O13	103.2 (3)	O20^{IV}—Mn3—O31A	86.8 (7)
O14—W4—O13	94.2 (3)	O31A^{IV}—Mn3—O31A	179.999 (1)
O15—W4—O8	97.4 (3)	O20—Mn3—O30A^{IV}	89.8 (8)
O14—W4—O8	92.3 (3)	O20^{IV}—Mn3—O30A^{IV}	90.2 (8)
O13—W4—O8	156.2 (3)	O31A^{IV}—Mn3—O30A^{IV}	92.0 (11)
O15—W4—O10	96.5 (3)	O31A—Mn3—O30A^{IV}	88.0 (11)
O14—W4—O10	160.0 (3)	O20—Mn3—O30A	90.2 (8)
O13—W4—O10	83.6 (2)	O20^{IV}—Mn3—O30A	89.8 (8)
O8—W4—O10	82.6 (2)	O31A^{IV}—Mn3—O30A	88.0 (11)
O15—W4—O6	165.1 (3)	O31A—Mn3—O30A	92.0 (11)
O14—W4—O6	87.1 (3)	O30A^{IV}—Mn3—O30A	179.999 (2)
O13—W4—O6	86.3 (2)	O20—Mn3—O31	89.2 (3)
O8—W4—O6	71.2 (2)	O20^{IV}—Mn3—O31	90.8 (3)
O10—W4—O6	72.9 (2)	O30^{IV}—Mn3—O31	89.7 (4)
O21—W5—O20	102.5 (3)	O30—Mn3—O31	90.3 (4)
O21—W5—O11	100.6 (3)	O20—Mn3—O31^{IV}	90.8 (3)
O20—W5—O11	97.9 (3)	O20^{IV}—Mn3—O31^{IV}	89.2 (3)
O21—W5—O16	96.4 (3)	O30^{IV}—Mn3—O31^{IV}	90.3 (4)

O20—W5—O16	95.6 (3)	O30—Mn3—O31^{iv}	89.7 (4)
O11—W5—O16	155.3 (3)	O31—Mn3—O31^{iv}	179.999 (1)
O21—W5—O19	87.4 (3)	W2—O1—W1	140.8 (3)
O20—W5—O19	169.5 (3)	W2—O1—W6^{i}	124.2 (3)
O11—W5—O19	83.7 (2)	W1—O1—W6^{i}	93.3 (2)
O16—W5—O19	79.4 (2)	W1—O2—W3	148.4 (4)
O21—W5—O13	161.7 (3)	W6^{i}—O3—W1	117.2 (3)
O20—W5—O13	93.1 (3)	W1—O4—Mn2^{ii}	137.8 (4)
O11—W5—O13	86.4 (3)	W1—O5—Mn1	137.5 (3)
O16—W5—O13	72.4 (2)	W2—O6—W4	97.2 (3)
O19—W5—O13	76.6 (2)	W2—O6—W3	97.0 (2)
O17—W6—O18	102.6 (3)	W4—O6—W3	95.9 (2)
O17—W6—O3^{i}	99.9 (3)	W2—O8—W4	117.8 (3)
O18—W6—O3^{i}	98.6 (3)	W2—O9—Mn2	169.8 (4)
O17—W6—O16	100.7 (3)	W3—O10—W4	115.3 (3)
O18—W6—O16	95.3 (3)	W5—O11—W3	149.2 (4)
O3^{i}—W6—O16	151.9 (3)	W4—O13—W6	125.6 (3)
O17—W6—O13	96.6 (3)	W4—O13—W5	137.9 (3)
O18—W6—O13	159.8 (3)	W6—O13—W5	95.1 (2)
O3^{i}—W6—O13	84.3 (2)	W4—O14—W1^{i}	136.7 (3)
O16—W6—O13	74.5 (2)	W6—O16—W5	116.5 (3)
O17—W6—O1^{i}	170.9 (3)	W6—O18—Mn2^{v}	135.8 (4)
O18—W6—O1^{i}	84.3 (3)	W2^{i}—O19—W5	137.3 (3)
O3^{i}—W6—O1^{i}	72.9 (2)	W5—O20—Mn3	164.3 (4)

Table S3. BVS sums calculated for the Mn1-Mn3 atoms (for Mn3 bond lengths for the higher-occupancy disorder component are taken).

	Mn1	**Mn2**	**Mn3**
Mn^{II}	2.03	2.03	2.06
Mn^{III}	1.92	1.93	1.98
Mn^{IV}	1.95	1.95	1.98

Table S4. Parameters of hydrogen bonding involving the located H atoms [Å, °] for **1**. Symmetry codes: (i) -*x*, -*y*+1, -*z*+1; (ii) -*x*, -*y*+2, -*z*; (iii) -*x*+1, -*y*+1, -*z*+1.

D—H···*A*	*D*—H	H···*A*	*D*···*A*	*D*—H···*A*
O6—H6···O19	0.82	2.25	2.875 (9)	134
O6—H6···O14^{i}	0.82	2.24	2.859 (9)	132
O6—H6···O6^{i}	0.82	2.30	2.897 (12)	130
O1W—H1W1···O19	0.82	2.22	3.030 (11)	170
O1W—H2W1···O3W^{i}	0.82	2.25	2.888 (13)	135
O2W—H2W2···O9W	0.82	2.05	2.517 (17)	116
O2W—H2W2···O9W^{ii}	0.82	2.50	2.934 (18)	114
O2W—H2W2···O10W	0.82	2.55	2.936 (19)	111
O3W—H1W3···O77W^{iii}	0.82	2.33	2.95 (2)	134

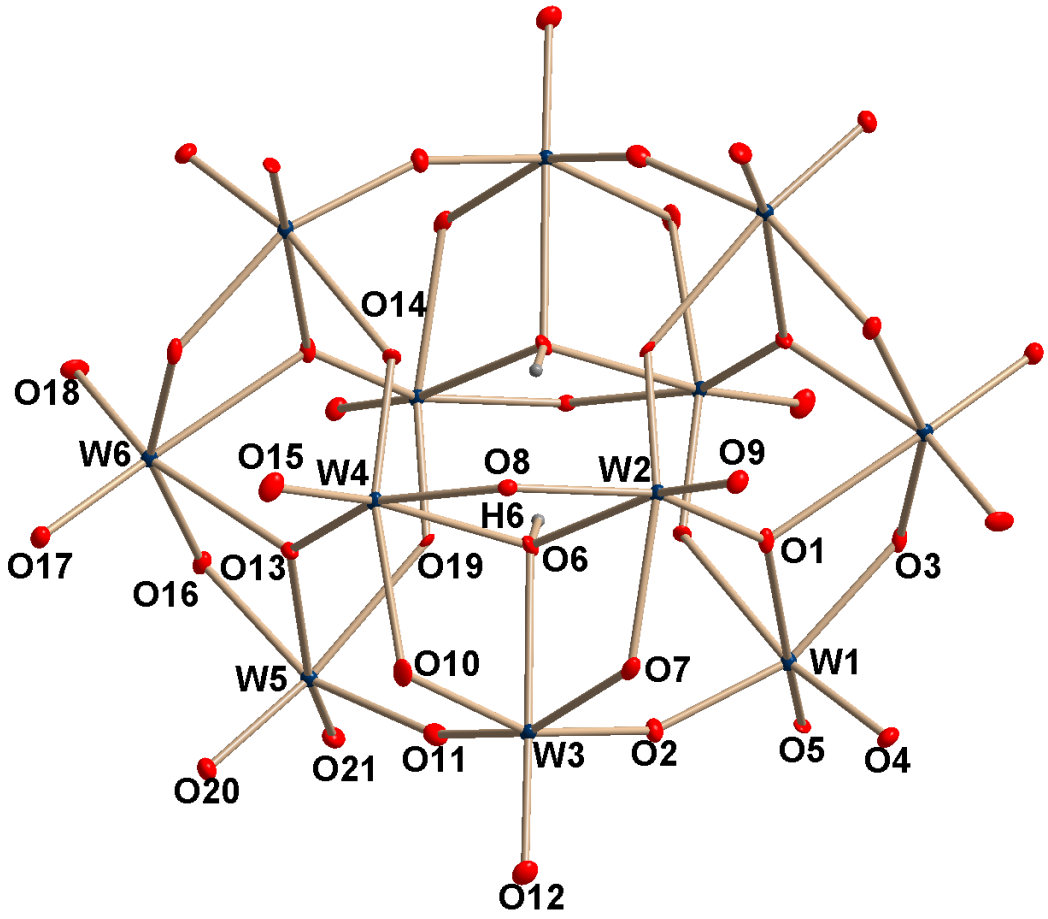

Fig. S12 Structure of the complex anion with atom labeling scheme of the symmetry-independent part. Thermal ellipsoids are plotted at 30% probability level.

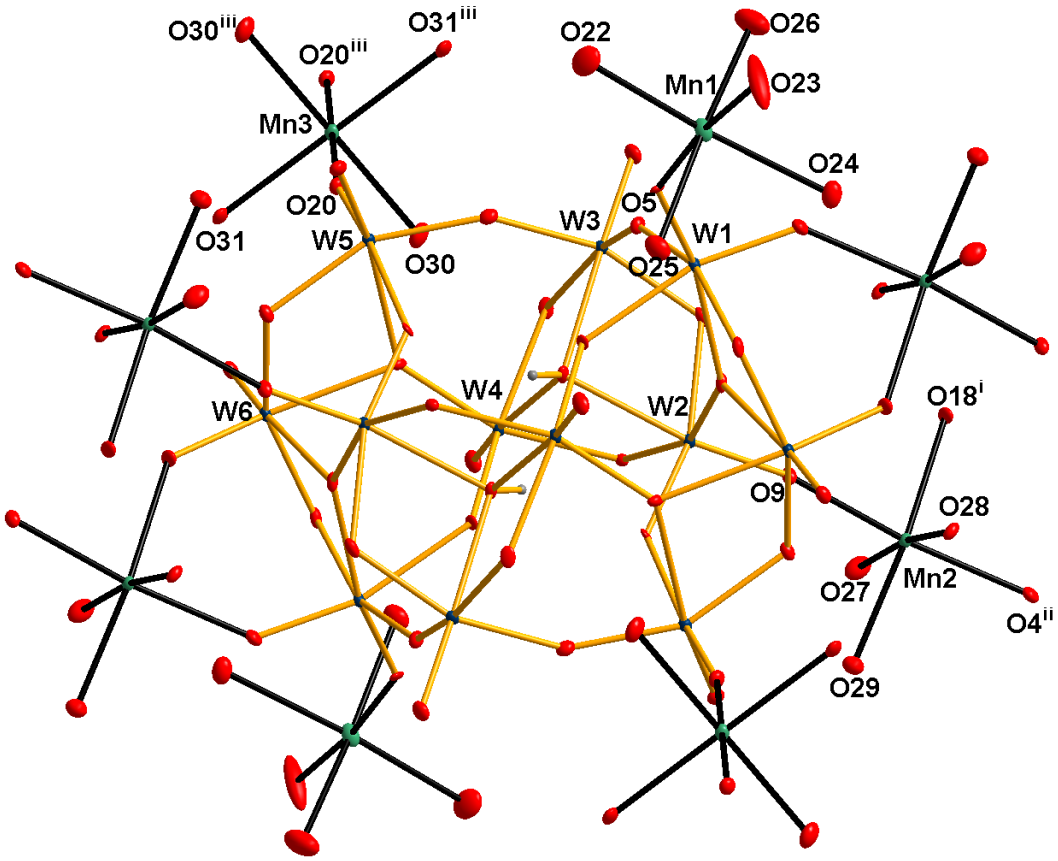

Fig. S13 Coordination of the Mn^{2+} ions to the complex anion with Mn-O bonds denoted with black lines and atom labeling scheme. Symmetry codes: [i] x, 1+y, z; [ii] –x, 2-y, 1-z; [iii] 1-x, 1-y, -z. Thermal ellipsoids are plotted at 30% probability level.

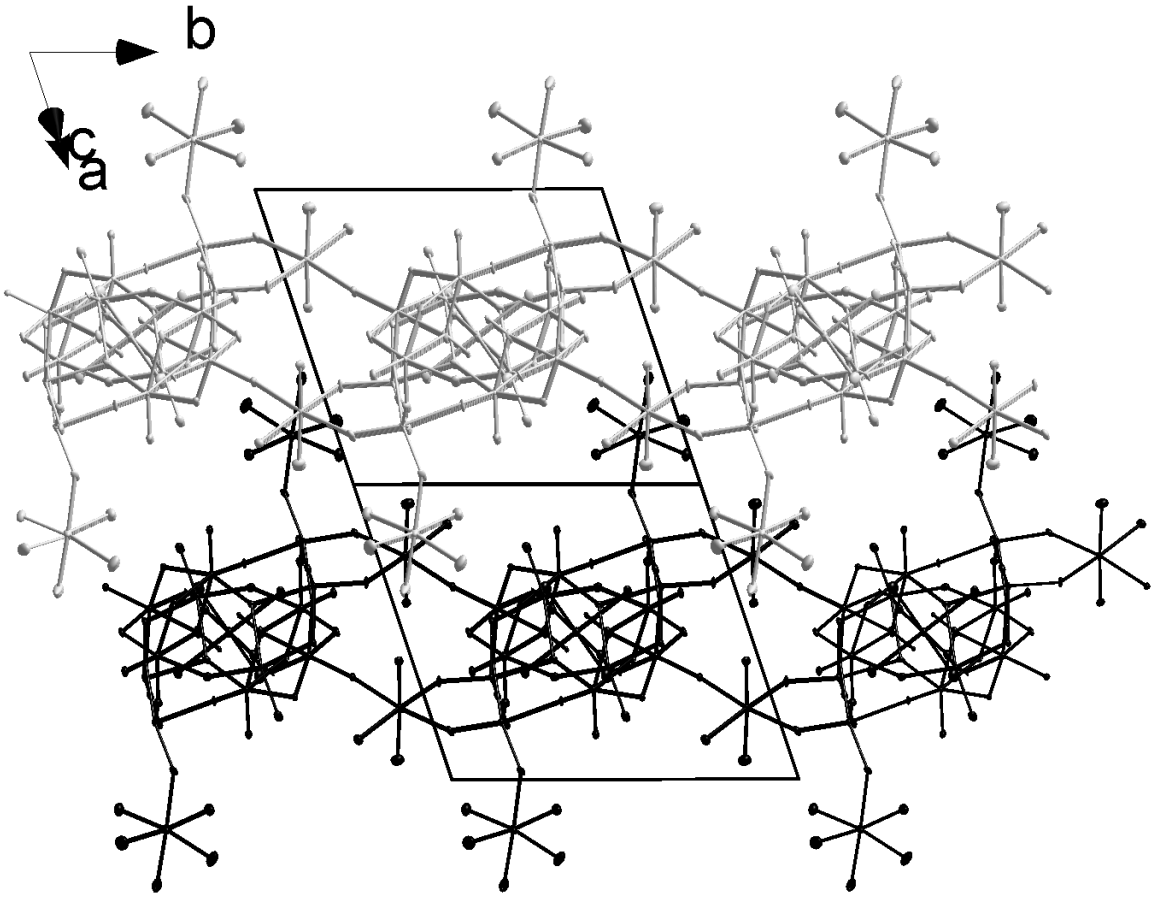

Fig. S14 Two-dimensional polymeric layers in **1** denoted with different colours. Water molecules of solvation are omitted for clarity.

EDX analysis

Energy dispersive X-ray (EDX) spectroscopy was performed for crystalline samples, using a CamScan 4DV device with EDX Noran Instruments Voyager 4.0 (Pioneer Detector with ultrathin window).

	k-ratio (calc.)	ZAF	Atom %	Element Wt %	Wt % Err (1-Sigma)
1: chi sqd. = 1.77					
Mn-K	0.1272	0.983	32.35	12.50	± 0.49
W-L	0.8390	1.043	67.65	87.50	± 2.24

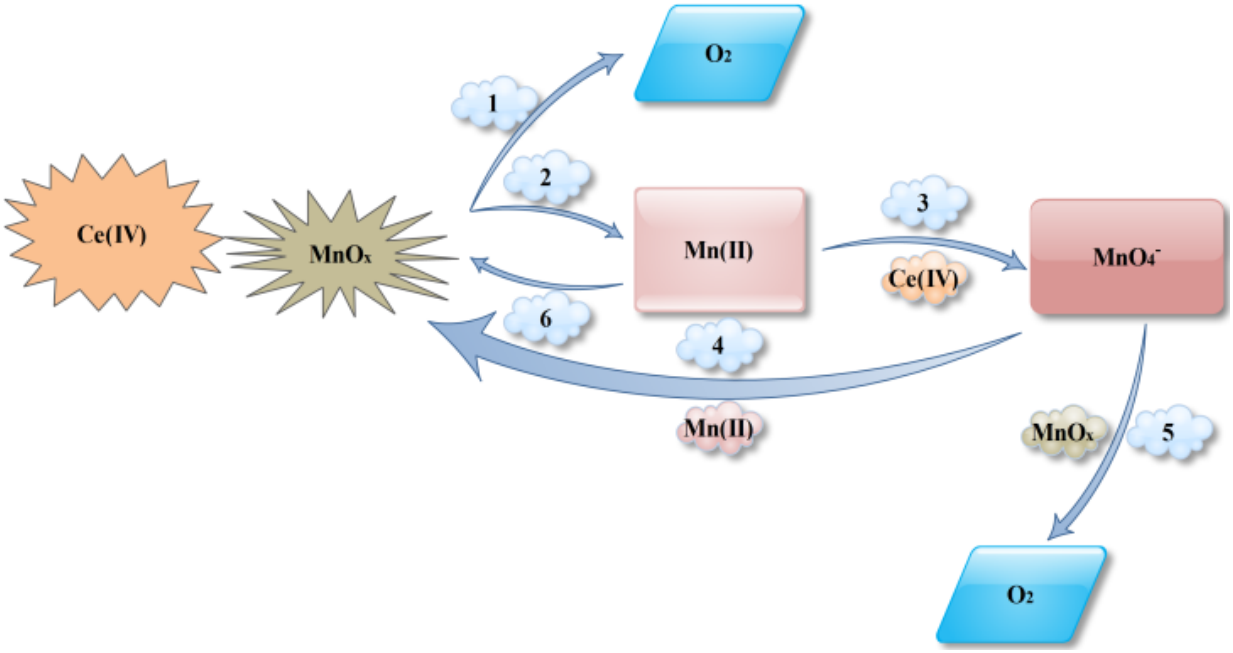

Scheme S1 Proposed mechanisms for the self-healing process in water oxidation catalyzed by Mn oxides in the presence of Ce(IV) 1: Oxygen evolution was detected by an oxygen meter. The origin of oxygen is water. 2: Mn^{2+} ions were detected by EPR (see text). 3: The MnO_4^- ions formation could be detected by UV-Vis in a reaction between Mn^{2+} and Ce(IV). 4: It is known that in the reaction of the Mn^{2+} ions and MnO_4^- in different pH values, Mn oxide is produced. 5: MnO_4^- in the presence of Mn oxide oxidize water. In this reaction, MnO_4^- ions are reduced to Mn oxide. 6: Mn^{2+} in the presence of Ce(IV) forms Mn oxide. In a typical experiment, the reaction of $MnSO_4$ in the presence of Ce(IV) (1.0 M), results in the MnO_2 product detected by XRD. Image and caption are taken from ref. S4 with modifications.

References

[S1] Y. Umena, K. Kawakami, J. R. Shen and N. Kamiya, *Nature*, 2011, **473**, 55.

[S2] K. J. Klabunde, J. Stark, O. Koper, C. Mohs, D. G. Park, S. Decker, Y. Jiang, I. Lagadic and D. Zhang, *J. Phys. Chem.*, 1996, **100**, 12142.

[S3] G. M. Sheldrick, SHELXTL 5.1, Bruker AXS Inc., 6300 Enterprise Lane, Madison, WI 53719-1173, USA, 1997.

[S4] M. M. Najafpour, M. Kompany-Zareh, A. Zahraei, D. Jafarian Sedigh, H. Jaccard, M. Khoshkam, R. D. Britt and W. Casey, 2013, **42**, 14603.